WHAT MAKES A GOOD DIFFUSION PLANNER FOR DECISION MAKING?

Anonymous authors
Paper under double-blind review

ABSTRACT

Diffusion models have recently shown significant potential in solving decision-making problems, particularly in generating behavior plans – also known as diffusion planning. While numerous studies have demonstrated the impressive performance of diffusion planning, the mechanisms behind the key components of a good diffusion planner remain unclear and the design choices are highly inconsistent in existing studies. In this work, we address this issue through systematic empirical experiments on diffusion planning in an offline reinforcement learning (RL) setting, providing practical insights into the essential components of diffusion planning. We trained and evaluated over 6,000 diffusion models, identifying the critical components such as guided sampling, network architecture, action generation and planning strategy. We revealed that some design choices opposite to the common practice in previous work in diffusion planning actually lead to better performance, e.g., unconditional sampling with selection can be better than guided sampling and Transformer outperforms U-Net as denoising network. Based on these insights, we suggest a simple yet strong diffusion planning baseline that achieves state-of-the-art results on standard offline RL benchmarks.

1 INTRODUCTION

Decision making by learning from offline data has been a fundamental approach in robotics and artificial intelligence (Bellman, 1957). It enables agents to acquire complex behaviors by observing and mimicking expert demonstrations, circumventing the need for explicit programming or exhaustive exploration. However, this paradigm faces significant challenges, particularly when dealing with long-horizon planning and high-dimensional action spaces. The complexity of modeling sequential dependencies and capturing the intricacies of action distributions makes it difficult to scale traditional methods (Deisenroth & Rasmussen, 2011) to more complex tasks (Parmas et al., 2018).

Recently, diffusion models have achieved remarkable success in image and video generation, demonstrating their ability to handle complex distribution and long-range dependencies (Ho et al., 2020; Dhariwal & Nichol, 2021). Inspired by these works, several recent studies have applied diffusion models to planning sequential decisions, especially with continuous state and action spaces such as robotic manipulation tasks (Janner et al., 2022; Ajay et al., 2022; Lu et al., 2023; Li et al., 2023). The diffusion models are used to approximate the sequence of states and actions from current time step to future – and by exploiting the diffusion models' conditional generation capacity such as diffusion guidance (Ho et al., 2020; Ho & Salimans, 2021), the model can make plans (i.e. state trajectory) with desired properties such as reward maximization (i.e. offline reinforcement learning (Levine et al., 2020)).

Despite achieving impressive performance across a diverse array of tasks, there has been limited exploration into the fundamental components and mechanisms that constitute an effective diffusion planning model for decision making. Previous research exhibits a lack of consistency and coherence in design choices. It remains uncertain whether sub-optimal design choices might hinder the full potential of diffusion models within decision-making domains. Specifically, existing approaches have not adequately addressed essential facets such as the choice of diffusion guidance algorithm, network architecture, and whether the plan should contain states or state-action pairs. This naturally raises the following fundamental question:

What makes a good diffusion planner for decision making, especially offline RL?

We seek to answer the question by conducting a comprehensive empirical investigation into key design choices in diffusion models for decision-making, in particular for state-based robotics tasks. Our work contributes to the field of decision making and diffusion models in several aspects.

- **Comprehensive Experiments:** We conducted an extensive empirical study to explore what constitutes an effective diffusion planner. By training and evaluating over 6,000 models, we analyzed key components critical to decision making in diffusion planning, including guided sampling algorithms, network architectures, action generation methods, and planning strategies.
- **Insights and Tips:** We ran detailed experiments and data analysis to understand the role of each key component in constituting a good diffusion planner. In particular, we discovered that certain design choices, contrary to common practice in diffusion planning actually lead to better performance. Our work offers intuitive explanations and practical tips about the choices and provides insights about the strengths and limitations of diffusion planning.
- **A simple yet strong baseline:** Building on the insights from our study, we suggest a simple yet highly competitive baseline, named *Diffusion Veteran* (DV). This model achieves state-of-the-art performance in planning tasks in standard offline RL benchmarks.

2 Background and Related Work

Offline Reinforcement Learning (Fujimoto et al., 2019; Levine et al., 2020; Fu et al., 2020) is a subfield of reinforcement learning (RL) where the agent learns from a fixed dataset of past experiences. This dataset typically consists of state-action-reward-next-state tuples, which encapsulate the agent's interactions with the environment. The challenge in offline RL is for the agent to derive an effective policy from this static dataset without further exploration or interaction with the environment. Two major challenges arise in this context. First, the state and action spaces may be high-dimensional and involve long-range dependencies, making it difficult to model effectively (Levine et al., 2020). Second, the learned policy must be optimal, even though the behavior policy that generated the offline data may be sub-optimal or different from the desired policy (Fujimoto et al., 2019).

Recently, diffusion models have emerged as a powerful framework for tasks such as image and video generation due to their ability to model complex distributions (Croitoru et al., 2023), which could mitigate the first problem. Moreover, diffusion guidance techniques (Ho et al., 2020; Ho & Salimans, 2021) allow the model to generate samples that adhere to the desired properties. The second challenge in offline RL, learning an optimal policy, can be addressed by diffusion guidance techniques to produce behavior that maximizes rewards. Building on this insight, a growing body of research has explored the use of diffusion models to generate behavior trajectories, denoted as τ.

Diffusion planning (Ajay et al., 2022; Janner et al., 2022; Liang et al., 2023; Dai et al., 2023; Yang et al., 2023; Li et al., 2023; Yang et al., 2023; Chen et al., 2024; Dong et al., 2024c) considers that at the time step t, a *trajectory* τ consists of the current and subsequent H steps of state-action pairs or states:

$$\tau = \begin{bmatrix} s_t & s_{t+1} & \cdots & s_{t+H-1} \\ a_t & a_{t+1} & \cdots & a_{t+H-1} \end{bmatrix}, \text{ or } \tau = \begin{bmatrix} s_t & s_{t-1} & \cdots & s_{t+H-1} \end{bmatrix}. \tag{2.1}$$

There is a guidance function to model the reward, such as the immediate reward r_t or the state value function $v(s_t) = \mathbb{E}\left[\sum_{h=0}^{\text{end}} \gamma^h r_{t+h}\right]$, where γ is the discount factor (Sutton & Barto, 1998). In classifier guidance (CG) (Ho et al., 2020), a guidance network is learned simultaneously with the diffusion model, whose input is the generated trajectory and the output is accumulated rewards or value function. The gradient of the guidance network is used in the generation process of diffusion model to maximize the rewards. Examples of diffusion planning with CG are (Janner et al., 2022; Liang et al., 2023; Zhang et al., 2022) In classifier-free guidance (CFG) (Ho & Salimans, 2021), it takes the desired reward or value function as an additional argument feed into the diffusion process. Instances are (Ajay et al., 2022; Li et al., 2023; Yang et al., 2023). However, despite some literature reviews such as Zhu et al. (2023), **the field lack a systematical study to elucidate the design space of diffusion planning in offline RL with substantial experimental results.**

Diffusion policy (Pearce et al., 2023; Wang et al., 2023b; Hansen-Estruch et al., 2023; Chen et al., 2023) is another kind of popular usage of diffusion model in decision making. The trajectory only

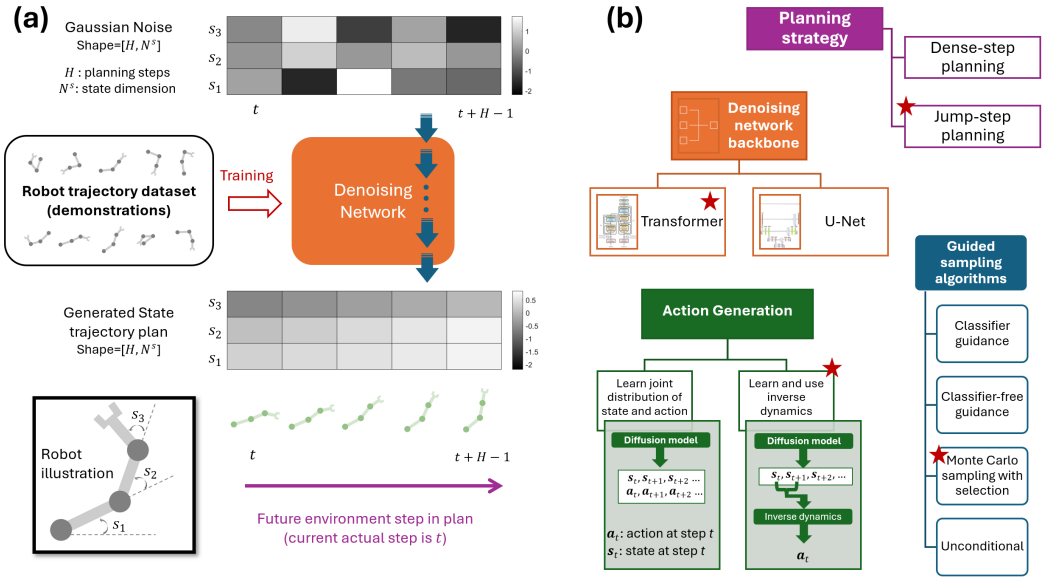

Figure 1: **Diffusion planning framework for decision making.** (**a**) The generation of a sequence plan using the denoising process of a diffusion model. A 3-joints robot arm is used as an illustrative example. (**b**) Important components and candidates in the framework. Each color corresponds to one component in the framework. A star indicates the preferred choice in experiments.

includes $\tau = a_t$, without lookahead planning. The model is trained by combining the loss of imitation learning and model-free RL as in classic offline RL methods (Kumar et al., 2020; Fujimoto & Gu, 2021). Diffusion policy methods hope to improve the performance of by leveraging the capacity of diffusion model to model complex distribution of actions (policy function). A recent study (Dong et al., 2024b) investigated the design space of diffusion policy, proposed that diffusion policies such as DQL (Wang et al., 2023b) can be a computationally efficient and powerful candidate for decision-making tasks.

3 Study Design

3.1 Key components and mechanisms of diffusion planner

Recent pioneering work in diffusion planning (Janner et al., 2022; Ajay et al., 2022; Chen et al., 2024) has demonstrated the potential of this approach in offline RL. However, the design choices in these studies vary significantly, and it remains unclear whether there is an optimal configuration for different domains. Our aim is to conduct a systematic analysis supported by comprehensive experimental results. To achieve this, we begin by listing key design components (excluding common deep learning hyperparameters such as learning rates) that have varied in previous studies. See Fig. 1(b) for an overview.

Guided sampling algorithms: Classifier guidance (CG) (Ho et al., 2020), Classifier-free guidance (CFG) (Ho & Salimans, 2021), Monte Carlo sampling with selection (sample N *unconditional* trajectories and select the best, the criteria of which is given by a critic function learned simultaneously with diffusion model). Most previous diffusion planners used CG (Janner et al., 2022; Wang et al., 2023a; Chen et al., 2024) or CFG (Ajay et al., 2022; Li et al., 2023; Yang et al., 2023) for offline RL.

Denoising network backbone: U-Net (Ronneberger et al., 2015); Transformer (Vaswani et al., 2017). U-Net was used in most previous diffusion planners for state-based offline RL (Janner et al., 2022; Ajay et al., 2022; Wang et al., 2023a; Li et al., 2023; Chen et al., 2024))

Action Generation: Learn joint distribution of state and action and directly execute the generated action at the current step (used in, e.g. Janner et al. (2022); Liang et al. (2023)); Learn and use inverse dynamics to compute action from state plan (used in e.g., Ajay et al. (2022); Wang et al. (2023a)).

Planning strategy: Dense-step planning means the planned trajectory τ (Eq. 2.1) corresponds to contiguous H steps in the environment (this is a conventional setting in diffusion planning (Janner et al., 2022; Ajay et al., 2022; Lu et al., 2023)) ; Jump-step planning models $H \times m$ environment steps, where $m \in \mathbb{N}^+$ is the planning stride; Hierarchical planning (studied by Li et al. (2023); Chen et al. (2024)).

Details of the implementation are deferred to Appendix A and B.

3.2 Experiment procedure

Given the multitude of components involved, it is challenging to draw scientific conclusions directly from the collective results. Therefore, we structured our study using the following procedure:
(1) Conduct a comprehensive search on the key components (Sect. 3.1) by combining grid search and manual tuning to obtain the best results.
(2) Evaluate the effect of each component using the control variable method; that is, modify only one component of the best model at a time and compare it with the original.
(3) After identifying which components are important and understanding how they affect performance, perform a deeper analysis to derive useful insights.

3.3 Benchmark

We conducted experiments on the D4RL dataset (Fu et al., 2020), one of the most widely used benchmarks for offline RL and imitation learning. The dataset covers a variety of task domains, including maze navigation, robot locomotion, robot arm manipulation, and vehicle driving, among others. For our experiments, we selected three sets of behavior planning tasks that were most commonly studied in prior works in offline RL and diffusion planning (Janner et al., 2021; Ajay et al., 2022; Janner et al., 2022; Liang et al., 2023; Li et al., 2023; Lu et al., 2023; Chen et al., 2024). These tasks (Fig. 2) encompass both planning and control challenges, providing a comprehensive evaluation in various problem settings. The performance metric considered in this work is the standard RL objective: the average total rewards in an online testing episode.

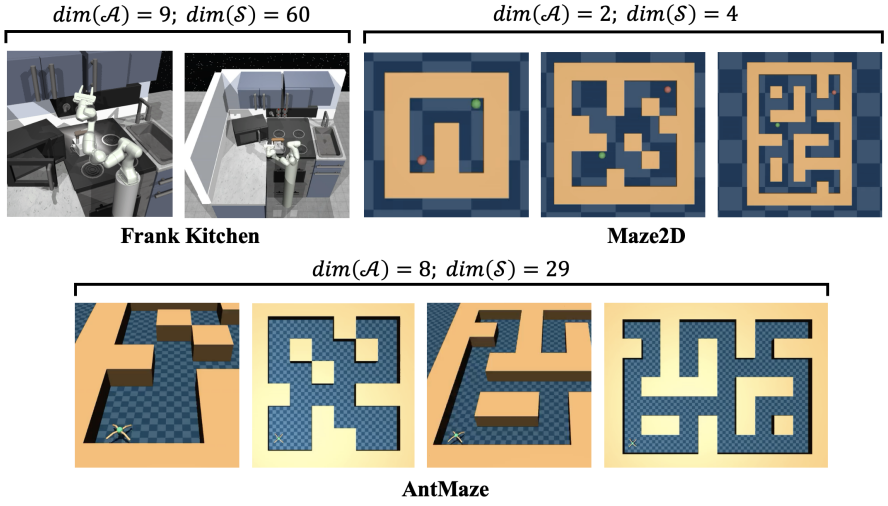

Figure 2: **Rendering of the benchmarking tasks considered in this study, where $dim(\mathcal{S})$ and $dim(\mathcal{A})$ denote the dimension of the state and action spaces.**

Maze2D involve navigating a 2D maze, requiring the agent to find an optimal path to a goal. These tasks are used to test planning capabilities in environments where spatial reasoning is critical.

AntMaze presents a navigation challenge with a simulated ant robot. The agent controls a multi-legged robot to navigate through a 2D maze, combining both locomotion and planning.

Franka Kitchen simulates a robot arm performing a variety of manipulation tasks in a kitchen environment to achieve task goals across multiple stages.

	Env	Kitchen			Antmaze					Maze2D			
Category	**Dataset**	Mixed	Partial	**avg.**	L.-div.	L.-play	M.-div.	M.-play	**avg.**	L.	M.	Umaze	**avg.**
Non-diffusion	BC	47.5	33.8	40.7	0.0	0.0	0.0	0.0	0.0	5	30.3	3.8	13.0
	BCQ	8.1	18.9	13.5	2.2	6.7	0.0	0.0	2.2	6.2	8.3	12.8	9.1
	CQL	51.0	49.8	50.4	61.2	53.7	15.8	14.9	36.4	12.5	5.0	5.7	7.7
	IQL	51.0	46.3	48.7	47.5	39.6	70.0	71.2	57.1	58.6	34.9	47.4	47.0
Diffusion Policies	SfBC	45.4	47.9	46.7	45.5	59.3	82.0	81.3	67.0	74.4	73.8	73.9	74.0
	DQL	62.6	60.5	61.6	56.6	46.4	78.6	76.6	64.6	–	–	–	
	DQL*	55.1	65.5	60.3	70.6	81.3	82.6	87.3	80.5	186.8	152.0	140.6	159.8
	IDQL	66.5	66.7	66.6	67.9	63.5	84.8	84.5	75.2	90.1	89.5	57.9	79.2
	IDQL*	66.5	66.7	66.6	40.0	48.7	83.3	67.3	59.8	–	–	–	
	CEP	–	–	–	64.8	66.6	83.8	83.6	74.7	–	–	–	
Diffusion Planners	Diffuser	52.5	55.7	54.1	27.3	17.3	2.0	6.7	13.3	123	121.5	113.9	119.5
	AdpDfsr	51.8	55.5	53.7	8.7	5.3	6.0	12.0	8.0	167.9	129.9	135.1	144.3
	DD	75.0	56.5	65.8	0.0	0.0	4.0	8.0	3.0	–	–	–	
	HD	71.7	73.3	72.5	83.6	–	88.7	–	–	128.4	135.6	155.8	139.9
	DV (Ours)	73.6	94.0	**83.8**	80.0	76.4	87.4	89.0	**83.2**	203.6	150.7	136.6	**163.6**

Table 1: **Normalized performance of various offline-RL methods.** Our results (DV) are averaged over 500 episode seeds. The results of other methods are obtained from literature. We omit the variance over seeds for simplicity; however, it can be found in the detailed tables in Appendix C. The best average performance on each task set are marked in bold fonts. BC: vanilla imitation learning, BCQ: Fujimoto et al. (2019), CQL: Kumar et al. (2020), IQL: Kostrikov et al. (2021), SfBC: Chen et al. (2023), DQL: Wang et al. (2023b), IDQL: Hansen-Estruch et al. (2023), DQL* and IDQL*: replicated by Dong et al. (2024b), CEP: Lu et al. (2023), Diffuser: Janner et al. (2022), AdptDfsr: Liang et al. (2023), DD: Ajay et al. (2022), HD: Chen et al. (2024).

4 Experimental Results

We trained and evaluated over 6,000 diffusion models by sweeping the key components discussed in Sect. 3.1 and other hyper-parameters (See Appendix B for details).

By summarizing the results from the experiments, we identified one kind of diffusion planning framework, called the Diffusion Veteran (DV). The pseudocode of DV can be found in Algorithm 1. As shown in Table 1, DV outperforms all previous diffusion planning and diffusion policy methods. We hope DV will serve as a simple yet strong baseline for future research in diffusion planning.

Algorithm 1: Diffusion Veteran (DV) Simplified Pseudocode

Input: Planning horizon H, Dataset $\mathcal{D}$, Discount factor γ, Candidate num N, Planning stride M.
Initialize : Diffusion Transformer Planner ϵ_θ, Diffusion Inverse dynamics ϵ_ω, Critic V_ϕ

Calculate accumulated discounted returns $R_t = \sum_{h=0}^{\text{end}} \gamma^h r_{t+h}$ for every step t.
Function Training**:**
  Sample $\boldsymbol{s}_{t,t+M,\cdots,t+(H-1)M}, \boldsymbol{a}_{t,t+M,\cdots,t+(H-1)M}, R_t$ from $\mathcal{D}$
  Train planner ϵ_θ using $\boldsymbol{s}_t$ as condition and $\boldsymbol{s}_{t,t+M,\cdots,t+(H-1)M}$ as target output
  Train Inverse dynamics ϵ_ω using $\boldsymbol{s}_t, \boldsymbol{s}_{t+M}$ as input, $\boldsymbol{a}_t$ as target output
  Train critic V_ϕ using $\boldsymbol{s}_{t,t+M,\cdots,t+(H-1)M}$ as input, R_t as target output
end
Function Execution$(\boldsymbol{s})$**:**
  Randomly generate N plans using ϵ_θ, while fixing the first state as $\boldsymbol{s}$ during sampling
  Select the best plan using critic V_ϕ
  Use the inverse dynamics ϵ_ω to generate action using $\boldsymbol{s}$ and the next state in the best plan
end

With DV in place, we can then analyze the impact of each component in diffusion planning by looking into how each component influences its performance. Each of the following sub-sections will focus on one component that we have found to be crucial. In the end of this section, we will conclude our findings into practical tips.

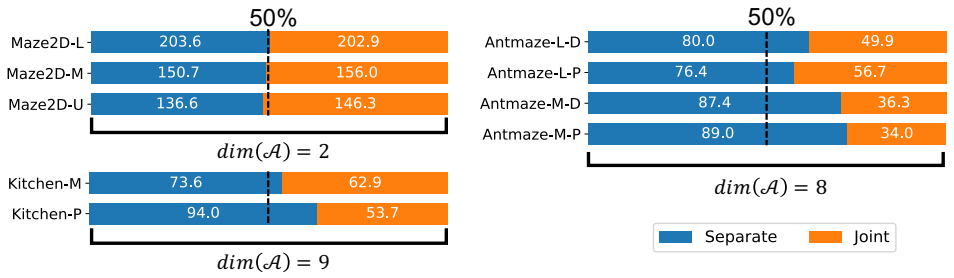

Figure 3: **Comparison of performance between two action generation strategies.** "Seperate" learns and uses inverse dynamics to compute action from state plan. "Joint" means learning joint distribution of state and action and directly executing the generated action at the current step (see "action generatation" in Fig. 1(b)). A straightforward conclusion drawn from the results is that "separate" is better than "Joint" when tackling higher-dimensional action spaces. The vertical dashed line indicates on-par performance.

4.1 Action Generation

The choice of action generation design (Sect. 3.1) remains a subject of ongoing debate within the field. On one side, the pioneering diffusion planner, Diffuser, along with subsequent studies (Janner et al., 2022; Liang et al., 2023; Chen et al., 2024), employs a diffusion model to generate the joint distribution of action and state trajectories ("joint"). In contrast, studies by Ajay et al. (2022); Wang et al. (2023a); Du et al. (2024) have adopted inverse dynamics to generate actions based on planned states ("separate").

Our experimental findings favor the latter approach: Although both strategies perform comparably in simpler environments such as Maze2D, which lacks robotic control elements, the "separate" approach significantly outperforms the "joint" strategy in more complex settings like Kitchen and AntMaze, which feature robotic control and higher-dimensional action spaces.

This observed disparity may be attributed to the additional complexity introduced when modeling the joint distribution of sequential states and actions, compared to modeling only the states. This complexity becomes particularly pronounced in environments where state transitions involve more complex actions due to higher-dimensional action spaces.

We tested both diffusion models and vanilla MLP as the inverse dynamics, and found similar performance between them. We adhered to diffusion inverse dynamics (Appendix B.1).

4.2 Planning Strategy

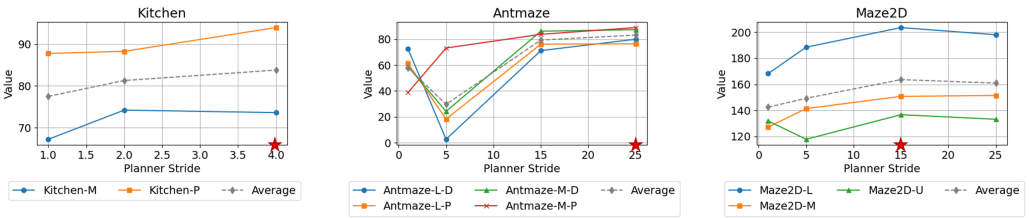

Figure 4: **Performance change of DV over planning stride**. It reduces to dense-step planning when Stride=1. The star indicates the choice of DV.

One crucial result we found is that jump-step planning (Sect. 3.1) is beneficial in almost all cases, despite the fact that most previous work used dense-step planning. This is observed in DV (Fig. 4) and generally in diffusion planners (see Appendix C for extensive results).

An obvious benefit from jump-step planning is that with the same planning steps, the model can look ahead farther. This may be crucial for planning tasks that require long-term credit assignment. The choice of stride should be related to the actual clock-time interval between two environment steps. Nonetheless, we suggest to try jump-steps and sweep the stride.

This observed phenomenon also implies that the diffusion planner should play the role of planning at a more abstract level or with a longer timescale. Interestingly, this is consistent with the neuroscientific fact that the intrinsic timescale of the prefrontal cortex (higher-level planning) is longer than that of the motor cortex (low-level control) (Murray et al., 2014; Runyan et al., 2017; Wang et al., 2018). A recent study (Chen et al., 2024) demonstrated impressive planning performance (Table 1, HD) using multi-timescale diffusion planning. Exploring the hierarchical paradigm of diffusion planning could be an interesting future direction.

4.3 Denoising Network Backbone

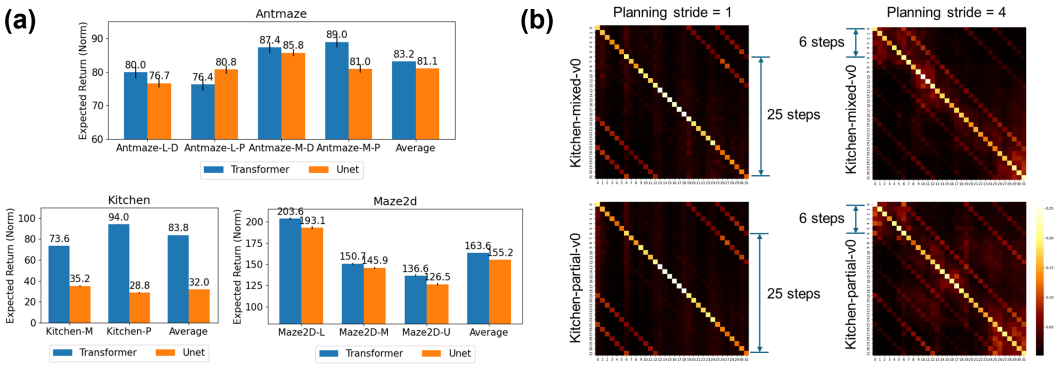

Figure 5: Using Transformer as the backbone of denoising network. (**a**) Performance comparison between Transformer and U-Net.The Transformer outperforms U-Net in 8 out of 9 sub-tasks and in all 3 main tasks. The amount of parameters in U-Net is comparable to that in Transformers. (**b**) Visualization of attention weights of the first layer in the Transformer network during the denoising process. More plots can be found in Appendix C.

Most diffusion planners on the D4RL dataset use 1-D U-Net for the denoising network. It is natural to question whether attention is all you need (Vaswani et al., 2017) for diffusion planning. Thus, we examined the benefit of replacing U-Net with the Transformer architecture as the backbone of the denoising model (Sect. 3.1) (see Appendix B for details about network structures). The experimental results clearly support the utilization of Transformer (Fig. 5(a)) in diffusion planning, consistent with the latest trend in image and video generation (Peebles & Xie, 2023; OpenAI, 2024).

We also conducted a case study by looking into the attention weights of the trained Transformer in the Kitchen environment (Fig. 5(b)), which reflect the temporal credit assignment (i.e., to how many steps later should be paid attention in the planning sequence). First, we see that the model pays more attention to the long-range element in the trajectory compared to the short-range ones. It suggests that the long-term dependency is crucial in this task, which breaks the local inductive bias of convolutional neural networks such as U-Net. Second, an interesting finding is that the characteristic attention length is consistent even with different planning stride (Sect. 4.2): 6 (attention step) $\times$ 4 (stride) $\approx$ 25 (attention step) $\times$ 1 (stride), as depicted in Fig. 5(b). It suggests that the Transformer finds the invariant correlations across the stride, contributing to the generalization performance. We have included more attention weights visualization in Appendix C, which also implies the importance of long-term dependency in trajectory modeling. In-depth study will be needed to fully understand the long-term dependency in the future.

4.4 Impact of Network Size

Since the experimental results are in favor of Transformer, one may wonder whether a "scaling law" (Kaplan et al., 2020) holds, in particular, whether performance scales up with model depth (Ye et al., 2024). The results presented in Fig. 6 pass two clear messages: First, 1-layer Transformer is not

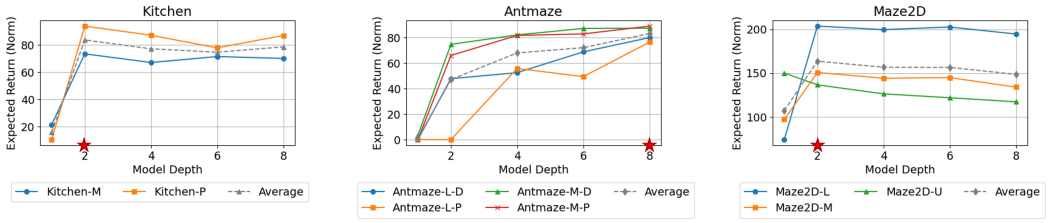

Figure 6: **Performance change over depth of the Transformer network as diffusion planner.** The star indicates the choice of DV.

enough, except for the simplist sub-task (Maze2D-U). Second, a deeper model is not always better. This may be due to a intrinsic difference between decision making and natural language processing and limitations of dataset size and quality, which requires further study to systematically address.

4.5 Guided Sampling Algorithms

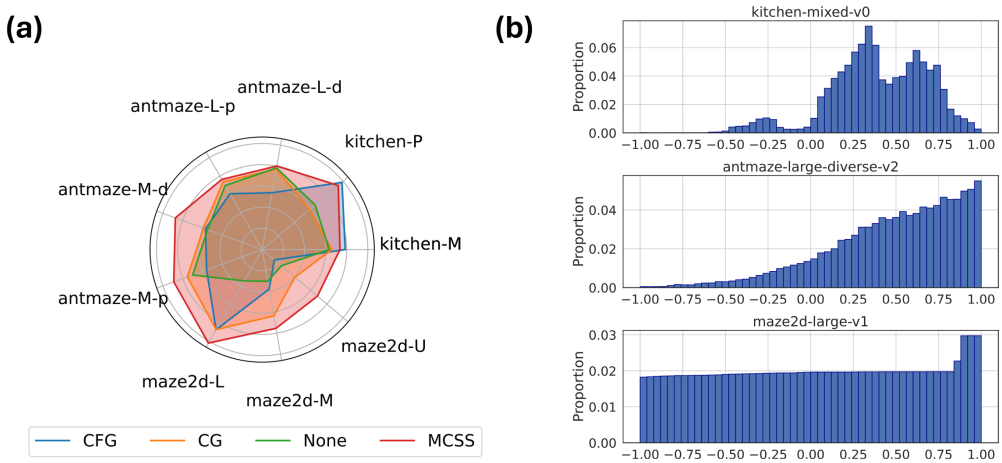

Figure 7: **Analysis of guided sampling algorithm.** (**a**) Performance comparison among different guided sampling algorithms for reward maximization. (**b**) Histogram of the value (accumulated discounted return in the future ($\sum_{h=0}^{\text{end}} \gamma^h r_{t+h}$, normalized to $[-1, 1]$) of the data points in each environment. For AntMaze, the failed trajectories are omitted since their values are all 0.

Another inconsistent design in previous work lies in the choice of guided sampling algorithm (Sect. 3.1), which enables the diffusion planner to generate plans that perform better than the average level of the dataset. Fig. 7(a) visualizes the corresponding empirical results (normalized) in our model. We can draw several conclusions from the results.

First, classifier guidance (CG) is comparable with classifier-free guidance (CFG), despite the fact that CFG is generally considered better than CG in image synthesis (Ho & Salimans, 2021). A potential reason is that the target value of CFG may need to be adjusted over time since the total rewards an agent can obtain in the future may vary depending on the task stage, but we can only use a fixed target value for CFG since there is no trivial solution.

Also, we observed that non-guidance can be better than guidance – Monte Carlo sampling with selection (MCSS) performs overall the best, except for Franka Kitchen where MCSS lags slightly behind CFG. This is an important finding since existing diffusion planners usually used CG or CFG (Chen et al., 2023; Wang et al., 2023b)). To understand the potential underlying reasons, we plotted the value distribution of data in each environment (Fig. 7(b)). It can be seen that in Maze2D and AntMaze, there is a substantial amount of optimal and near-optimal experiences, whereas in Kitchen

most samples are sub-optimal (note that here the optimality is with respect to condition of diffusion model). This may explain why CFG performs better than MCSS in Kitchen. Thus we can propose a hypothesis: No guidance (MCSS) can be better than guided generation (CG, CFG) if the dataset contains a substantial portion of expert demonstration.

4.6 Comparison to diffusion policy

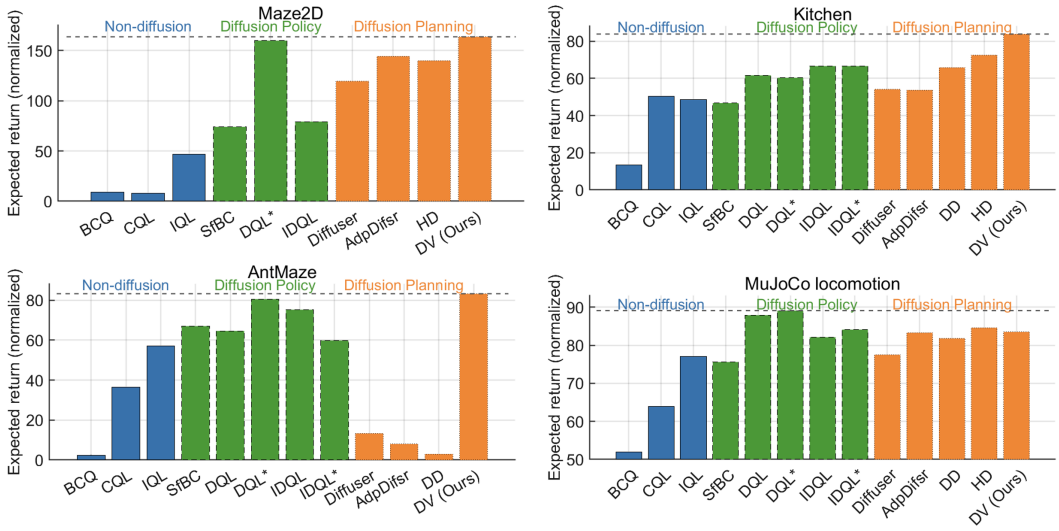

Figure 8: **Average performance of methods on different tasks.** The horizontal dashed line indicates the best performance over all methods. DV (Diffusion planning) shows the best performance for Kitchen, Maze2D, and AntMaze; while DQL (Diffusion policy) (Wang et al., 2023b) outperforms all diffusion planning methods in MuJoCo locomotion tasks. Refer to the caption of Table 1 for the reference of each method.

Diffusion planning and diffusion policy represent two key approaches within diffusion-based decision-making. After examining the core components of diffusion planners, we turn to a comparison of diffusion planning and diffusion policy across different environments. The experimental results are illustrated in Fig. 8. We observed that diffusion planning outperforms diffusion policy in AntMaze, Kitchen, and Maze2D, whereas diffusion policy excels in MuJoCo locomotion tasks. The first three environments require precise goal achievement, such as positioning an object exactly, necessitating long-term planning. This makes them well-suited to diffusion planning, which generates entire trajectories in one step. Furthermore, these environments feature sparse reward structures, posing challenges for model-free RL algorithms typically used in diffusion policies (Wang et al., 2023b). In contrast, the objective in MuJoCo is simply to control agents to run faster, a task that is less related to lookahead planning and does not require intricate planning. RL loss functions can help diffusion policy (Wang et al., 2023b) achieve better results in such scenarios.

4.7 Practical tips to take home

Takeaway 1: Diffusion planning is most effective for tasks requiring long-term credit assignment, while diffusion policies are better suited for locomotion tasks that do not demand long-term planning(Sect. 4.6)

Takeaway 2: It is recommended to generate state plans with diffusion planners and use an inverse dynamics model to compute the corresponding actions(Sect. 4.1).

Takeaway 3: Implementing jump-step planning can be highly beneficial; experimenting with different planning strides is encouraged(Sect. 4.2).

Takeaway 4: It is worth trying to use Transformer as the backbone of diffusion planner, especially in the tasks that require long-term lookahead planning (Sect. 4.3).

Takeaway 5: A single-layer Transformer is insufficient for effective planning (Sect. 4.4).

Takeaway 6: Larger models do not necessarily lead to better performance in diffusion planner for offline RL (Sect. 4.4).

Takeaway 7: Non-guidance approaches, such as Monte Carlo unconditional sampling with selection, can outperform classifier or classifier-free guidance when the dataset contains enough near-optimal trajectories (Sect. 4.5).

5 Discussions

Synergy between diffusion planning and diffusion policy. A significant avenue for future research involves a deeper exploration of the distinctions between diffusion planning and diffusion policy. Drawing on Daniel Kahneman's seminal work *Thinking, Fast, and Slow* (Kahneman, 2011), human cognitive processes are categorized into System 1 and System 2. Diffusion policies are analogous to System 1 processes, as they operate rapidly and efficiently (Wang et al., 2023b), making them well-suited for tasks such as locomotion (Fig. 8) that do not require extensive deliberation or long-term planning. These policies manage routine decision making with the same efficiency as intuitive responses in human cognition. Conversely, diffusion planning mirrors System 2 thinking, characterized by its slower, more deliberate, and effortful nature. This approach is particularly effective for tasks that demand long-term credit assignment (Fig. 8), involving more computations to develop effective plans. In RL terminology, diffusion planning can be broadly classified as model-based, while diffusion policy aligns with model-free methodologies. Investigating the interplay between these two systems presents a compelling intersection for both machine learning and cognitive neuroscience (Gläscher et al., 2010; Duan et al., 2016; Botvinick et al., 2019). Studies from cognitive science indicate that the brain may use a synergistic approach which arbitrates and selects the better system according to the current situation, and the preference may change over time (Lee et al., 2014; Han et al., 2024). We anticipate extensive future research focused on integrating the strengths of diffusion planning and diffusion policies to enable both efficient and effective decision-making AI.

Computational efficiency. Despite the effectiveness of diffusion planners, their computational cost is substantial. Our work is orthogonal to the optimization of computational cost (Dong et al., 2024a). Nonetheless, future work may consider new schemes such as the consistency model (Song et al., 2023) to improve computational efficiency.

Interpretability and safety. Our study focuses on a single performance metric (total return), potentially overlooking qualitative aspects such as the interpretability and reliability of the diffusion planner. Future work may consider issues such as explainability (Puiutta & Veith, 2020) and safety (Xiao et al., 2023) of diffusion planning. Leveraging the experiences from computer vision domain will be worth investigating.

Sustainability. Our work required significant computational resources, particularly in terms of GPU energy consumption, as we trained and evaluated thousands of models across diverse tasks. However, this investment in energy is not without purpose. We aim to provide a solid foundation for future research. Subsequent work can build upon our findings, reducing the need for extensive trial-and-error experimentation. In this way, our research contributes to energy efficiency in the long term, as researchers can reference our results and apply proven methods rather than duplicating resource-intensive exploratory efforts.

Open problems and future directions. In the current study, we have focused on standard Markov decision process problems (Bellman, 1957) using a popular offline RL benchmark (Fu et al., 2020). The planning and control are based on joint states and coordinates. Numerous untouched problems exist, such as vision-based decision making (Du et al., 2024; Yang et al., 2024), goal-conditioned reinforcement learning (Liu et al., 2022; Wang et al., 2023a), partially observable environments (Schmidhuber, 1991), offline-to-online deployment (Matsushima et al., 2021), and the scalability of diffusion planning models (Kaplan et al., 2020). Future efforts are anticipated to fully address these limitations. However, even within the scope of the current work, we have found several interesting phenomena and tips that are counter to common practices. Our work should be considered as a new but solid starting point for behavior planning using decision models.

Reproducibility Statement

We are committed to ensuring the reproducibility of our results. To facilitate this, we include the source code of DV in supplementary material and will release the code upon acceptance. Detailed descriptions of our experimental setup, including model architectures, training procedures, and hyperparameter settings, are provided in Appendix A and Appendix B. We have included comprehensive information on the datasets used, along with any preprocessing steps, in Appendix B. For all key experiments, we have specified the evaluation protocols and metrics in Sect. 3 and provided extensive results in Appendix C. We have included the full list of hyperparameters and configurations in Appendix B.4.

References

Anurag Ajay, Yilun Du, Abhi Gupta, Joshua B Tenenbaum, Tommi S Jaakkola, and Pulkit Agrawal. Is conditional generative modeling all you need for decision making? In *The Eleventh International Conference on Learning Representations*, 2022.

Richard Bellman. A Markovian decision process. *Journal of Mathematics and Mechanics*, pp. 679–684, 1957.

Matthew Botvinick, Sam Ritter, Jane X Wang, Zeb Kurth-Nelson, Charles Blundell, and Demis Hassabis. Reinforcement learning, fast and slow. *Trends in cognitive sciences*, 23(5):408–422, 2019.

Chang Chen, Fei Deng, Kenji Kawaguchi, Caglar Gulcehre, and Sungjin Ahn. Simple hierarchical planning with diffusion. *arXiv preprint arXiv:2401.02644*, 2024.

Huayu Chen, Cheng Lu, Chengyang Ying, Hang Su, and Jun Zhu. Offline reinforcement learning via high-fidelity generative behavior modeling. In *The Eleventh International Conference on Learning Representations*, 2023.

Florinel-Alin Croitoru, Vlad Hondru, Radu Tudor Ionescu, and Mubarak Shah. Diffusion models in vision: A survey. *IEEE Transactions on Pattern Analysis and Machine Intelligence*, 45(9): 10850–10869, 2023.

Yilun Dai, Mengjiao Yang, Bo Dai, Hanjun Dai, Ofir Nachum, Josh Tenenbaum, Dale Schuurmans, and Pieter Abbeel. Learning universal policies via text-guided video generation. *arXiv preprint arXiv:2302.00111*, 2023.

Marc Deisenroth and Carl E Rasmussen. Pilco: A model-based and data-efficient approach to policy search. In *Proceedings of the International Conference on Machine Learning*, pp. 465–472, 2011.

Prafulla Dhariwal and Alexander Nichol. Diffusion models beat gans on image synthesis. *Advances in neural information processing systems*, 34:8780–8794, 2021.

Zibin Dong, Jianye Hao, Yifu Yuan, Fei Ni, Yitian Wang, Pengyi Li, and Yan Zheng. Diffuserlite: Towards real-time diffusion planning. *arXiv preprint arXiv:2401.15443*, 2024a.

Zibin Dong, Yifu Yuan, Jianye Hao, Fei Ni, Yi Ma, Pengyi Li, and Yan Zheng. Cleandiffuser: An easy-to-use modularized library for diffusion models in decision making. *arXiv preprint arXiv:2406.09509*, 2024b.

Zibin Dong, Yifu Yuan, Jianye HAO, Fei Ni, Yao Mu, YAN ZHENG, Yujing Hu, Tangjie Lv, Changjie Fan, and Zhipeng Hu. Aligndiff: Aligning diverse human preferences via behavior-customisable diffusion model. In *The Twelfth International Conference on Learning Representations*, 2024c.

Yilun Du, Sherry Yang, Bo Dai, Hanjun Dai, Ofir Nachum, Josh Tenenbaum, Dale Schuurmans, and Pieter Abbeel. Learning universal policies via text-guided video generation. *Advances in Neural Information Processing Systems*, 36, 2024.

Yan Duan, John Schulman, Xi Chen, Peter L Bartlett, Ilya Sutskever, and Pieter Abbeel. RL2: Fast reinforcement learning via slow reinforcement learning. *arXiv preprint arXiv:1611.02779*, 2016.

Justin Fu, Aviral Kumar, Ofir Nachum, George Tucker, and Sergey Levine. D4rl: Datasets for deep data-driven reinforcement learning, 2020.

Scott Fujimoto and Shixiang Shane Gu. A minimalist approach to offline reinforcement learning. *Advances in neural information processing systems*, 34:20132–20145, 2021.

Scott Fujimoto, David Meger, and Doina Precup. Off-policy deep reinforcement learning without exploration. In *International Conference on Machine Learning*, pp. 2052–2062. PMLR, 2019.

Jan Gläscher, Nathaniel Daw, Peter Dayan, and John P O'Doherty. States versus rewards: dissociable neural prediction error signals underlying model-based and model-free reinforcement learning. *Neuron*, 66(4):585–595, 2010.

Dongqi Han, Kenji Doya, Dongsheng Li, and Jun Tani. Synergizing habits and goals with variational bayes. *Nature Communications*, 15(1):4461, 2024.

Philippe Hansen-Estruch, Ilya Kostrikov, Michael Janner, Jakub Grudzien Kuba, and Sergey Levine. Idql: Implicit q-learning as an actor-critic method with diffusion policies. *arXiv preprint arXiv:2304.10573*, 2023.

Jonathan Ho and Tim Salimans. Classifier-free diffusion guidance. In *NeurIPS 2021 Workshop on Deep Generative Models and Downstream Applications*, 2021.

Jonathan Ho, Ajay Jain, and Pieter Abbeel. Denoising diffusion probabilistic models. *Advances in neural information processing systems*, 33:6840–6851, 2020.

Michael Janner, Qiyang Li, and Sergey Levine. Offline reinforcement learning as one big sequence modeling problem. In *Advances in Neural Information Processing Systems*, volume 34, 2021.

Michael Janner, Yilun Du, Joshua Tenenbaum, and Sergey Levine. Planning with diffusion for flexible behavior synthesis. In *International Conference on Machine Learning*, pp. 9902–9915. PMLR, 2022.

Daniel Kahneman. *Thinking, fast and slow*. macmillan, 2011.

Jared Kaplan, Sam McCandlish, Tom Henighan, Tom B Brown, Benjamin Chess, Rewon Child, Scott Gray, Alec Radford, Jeffrey Wu, and Dario Amodei. Scaling laws for neural language models. *arXiv preprint arXiv:2001.08361*, 2020.

Diederik P Kingma and Jimmy Ba. Adam: A method for stochastic optimization. *arXiv preprint arXiv:1412.6980*, 2014.

Ilya Kostrikov, Ashvin Nair, and Sergey Levine. Offline reinforcement learning with implicit q-learning. *arXiv preprint arXiv:2110.06169*, 2021.

Aviral Kumar, Aurick Zhou, George Tucker, and Sergey Levine. Conservative q-learning for offline reinforcement learning. *Advances in Neural Information Processing Systems*, 33:1179–1191, 2020.

Sang Wan Lee, Shinsuke Shimojo, and John P O'Doherty. Neural computations underlying arbitration between model-based and model-free learning. *Neuron*, 81(3):687–699, 2014.

Sergey Levine, Aviral Kumar, George Tucker, and Justin Fu. Offline reinforcement learning: Tutorial, review, and perspectives on open problems. *arXiv preprint arXiv:2005.01643*, 2020.

Wenhao Li, Xiangfeng Wang, Bo Jin, and Hongyuan Zha. Hierarchical diffusion for offline decision making. In *International Conference on Machine Learning*, pp. 20035–20064. PMLR, 2023.

Zhixuan Liang, Yao Mu, Mingyu Ding, Fei Ni, Masayoshi Tomizuka, and Ping Luo. Adaptdiffuser: Diffusion models as adaptive self-evolving planners. *arXiv preprint arXiv:2302.01877*, 2023.

Minghuan Liu, Menghui Zhu, and Weinan Zhang. Goal-conditioned reinforcement learning: Problems and solutions. *arXiv preprint arXiv:2201.08299*, 2022.

Cheng Lu, Huayu Chen, Jianfei Chen, Hang Su, Chongxuan Li, and Jun Zhu. Contrastive energy prediction for exact energy-guided diffusion sampling in offline reinforcement learning. In *International Conference on Machine Learning*, pp. 22825–22855. PMLR, 2023.

Tatsuya Matsushima, Hiroki Furuta, Yutaka Matsuo, Ofir Nachum, and Shixiang Gu. Deployment-efficient reinforcement learning via model-based offline optimization. In *International Conference on Learning Representations*, 2021.

John D Murray, Alberto Bernacchia, David J Freedman, Ranulfo Romo, Jonathan D Wallis, Xinying Cai, Camillo Padoa-Schioppa, Tatiana Pasternak, Hyojung Seo, Daeyeol Lee, et al. A hierarchy of intrinsic timescales across primate cortex. *Nature Neuroscience*, 17(12):1661, 2014.

OpenAI. Sora. https://openai.com/index/sora/, 2024.

Paavo Parmas, Carl Edward Rasmussen, Jan Peters, and Kenji Doya. PIPPS: Flexible model-based policy search robust to the curse of chaos. In *International Conference on Machine Learning*, pp. 4065–4074. PMLR, 2018.

Tim Pearce, Tabish Rashid, Anssi Kanervisto, Dave Bignell, Mingfei Sun, Raluca Georgescu, Sergio Valcarcel Macua, Shan Zheng Tan, Ida Momennejad, Katja Hofmann, et al. Imitating human behaviour with diffusion models. *arXiv preprint arXiv:2301.10677*, 2023.

William Peebles and Saining Xie. Scalable diffusion models with transformers. In *Proceedings of the IEEE/CVF International Conference on Computer Vision*, pp. 4195–4205, 2023.

Erika Puiutta and Eric MSP Veith. Explainable reinforcement learning: A survey. In *International cross-domain conference for machine learning and knowledge extraction*, pp. 77–95. Springer, 2020.

Olaf Ronneberger, Philipp Fischer, and Thomas Brox. U-net: Convolutional networks for biomedical image segmentation. In *Medical Image Computing and Computer-Assisted Intervention–MICCAI 2015: 18th International Conference, Munich, Germany, October 5-9, 2015, Proceedings, Part III 18*, pp. 234–241. Springer, 2015.

Caroline A Runyan, Eugenio Piasini, Stefano Panzeri, and Christopher D Harvey. Distinct timescales of population coding across cortex. *Nature*, 548(7665):92, 2017.

Jürgen Schmidhuber. Reinforcement learning in Markovian and non-Markovian environments. In *Advances in Neural Information Processing Systems*, pp. 500–506, 1991.

Jiaming Song, Chenlin Meng, and Stefano Ermon. Denoising diffusion implicit models. *arXiv preprint arXiv:2010.02502*, 2020.

Yang Song, Prafulla Dhariwal, Mark Chen, and Ilya Sutskever. Consistency models. In *International Conference on Machine Learning*, pp. 32211–32252. PMLR, 2023.

Richard S Sutton and Andrew G Barto. *Reinforcement learning: An introduction*, volume 1. MIT press Cambridge, 1998.

Ashish Vaswani, Noam Shazeer, Niki Parmar, Jakob Uszkoreit, Llion Jones, Aidan N Gomez, Łukasz Kaiser, and Illia Polosukhin. Attention is all you need. In *Advances in Neural Information Processing Systems*, pp. 5998–6008, 2017.

Jane X Wang, Zeb Kurth-Nelson, Dharshan Kumaran, Dhruva Tirumala, Hubert Soyer, Joel Z Leibo, Demis Hassabis, and Matthew Botvinick. Prefrontal cortex as a meta-reinforcement learning system. *Nature Neuroscience*, 21(6):860, 2018.

Wei Wang, Dongqi Han, Xufang Luo, Yifei Shen, Charles Ling, Boyu Wang, and Dongsheng Li. Toward open-ended embodied tasks solving. In *Second Agent Learning in Open-Endedness Workshop*, 2023a.

Zhendong Wang, Jonathan J Hunt, and Mingyuan Zhou. Diffusion policies as an expressive policy class for offline reinforcement learning. In *The Eleventh International Conference on Learning Representations*, 2023b.

Wei Xiao, Tsun-Hsuan Wang, Chuang Gan, and Daniela Rus. Safediffuser: Safe planning with diffusion probabilistic models. *arXiv preprint arXiv:2306.00148*, 2023.

Cheng-Fu Yang, Haoyang Xu, Te-Lin Wu, Xiaofeng Gao, Kai-Wei Chang, and Feng Gao. Planning as in-painting: A diffusion-based embodied task planning framework for environments under uncertainty. *arXiv preprint arXiv:2312.01097*, 2023.

Sherry Yang, Yilun Du, Seyed Kamyar Seyed Ghasemipour, Jonathan Tompson, Leslie Pack Kaelbling, Dale Schuurmans, and Pieter Abbeel. Learning interactive real-world simulators. In *The Twelfth International Conference on Learning Representations*, 2024.

Tian Ye, Zicheng Xu, Yuanzhi Li, and Zeyuan Allen-Zhu. Physics of language models: Part 2.1, grade-school math and the hidden reasoning process. *arXiv preprint arXiv:2407.20311*, 2024.

Mingyuan Zhang, Zhongang Cai, Liang Pan, Fangzhou Hong, Xinying Guo, Lei Yang, and Ziwei Liu. Motiondiffuse: Text-driven human motion generation with diffusion model. *arXiv preprint arXiv:2208.15001*, 2022.

Zhengbang Zhu, Hanye Zhao, Haoran He, Yichao Zhong, Shenyu Zhang, Yong Yu, and Weinan Zhang. Diffusion models for reinforcement learning: A survey. *arXiv preprint arXiv:2311.01223*, 2023.

A GUIDED SAMPLING ALGORITHMS

For decision making tasks, guided sampling algorithms are used to generate desired plans or actions. In this work, we compare three types of different guided sampling methods: classifier guidance (Dhariwal & Nichol, 2021) (CG), classifier-free guidance (CFG) (Ho & Salimans, 2021), and Monte Carlo sampling from selections (MCSS).

Classifier guidance: Classifier guidance (CG) is introduced to guide the unconditional diffusion models $q_t(\boldsymbol{x}_t)$ to generate data over condition $\boldsymbol{c}$. The conditioned score function is formulated as:

$$\nabla_{\boldsymbol{x}} \log q_t(\boldsymbol{x}_t|\boldsymbol{c}) = \nabla_{\boldsymbol{x}} \log q_t(\boldsymbol{x}_t) + \nabla_{\boldsymbol{x}} \log q_t(\boldsymbol{c}|\boldsymbol{x}_t)$$

where the second term is also know as a noised classifier that predict the condition using noised data $\boldsymbol{x}_t$. During sampling, the gradient of the classifier is then applied to the predicted noise $\epsilon_\theta(\boldsymbol{x}_t, t)$:

$$\bar{\epsilon}_\theta(\boldsymbol{x}_t, t, \boldsymbol{c}) = \epsilon_\theta(\boldsymbol{x}_t, t) - w\sigma_t \nabla_{\boldsymbol{x}} \log q_t(\boldsymbol{c}|\boldsymbol{x}_t)$$

where w is a weighting factor that controls the strength of the classifier guidance. For CG sampling, we tuned w in range $[0.001, 10]$ on each task.

Classifier-free guidance: To avoid training classifiers, classifier-free guidance (CFG) is proposed. The main idea of CFG is to train a diffusion model that can be used for both conditional noise predictor $\epsilon_\theta(\boldsymbol{x}_t, t, \boldsymbol{c})$ and unconditional noise predictor $\epsilon_\theta(\boldsymbol{x}_t, t)$:

$$\bar{\epsilon}_\theta(\boldsymbol{x}_t, t, \boldsymbol{c}) = \epsilon_\theta(\boldsymbol{x}_t, t) + w(\epsilon_\theta(\boldsymbol{x}_t, t, \boldsymbol{c}) - \epsilon_\theta(\boldsymbol{x}_t, t))$$

where $\epsilon_\theta(\boldsymbol{x}_t, t) = \epsilon_\theta(\boldsymbol{x}_t, t, \varnothing)$. Noise prediction of $\epsilon_\theta(\boldsymbol{x}_t, t, \varnothing)$ and $\epsilon_\theta(\boldsymbol{x}_t, t, \boldsymbol{c})$ can be jointly learnt by randomly discard conditioning with probability of p_{uncond}. For decision making tasks, we can train diffusion models using condition of discounted returns, and using classifier-free guidance for better plan sampling. We can normalize the discounted return in the dataset for training, and use condition of 1 as target return for CFG sampling during inference (Ajay et al., 2022). However, experiments shows that fixing 1 as target may lead to unrealistic or unstable plans. Consequently, besides tuning the guidance strength $w \in [1.0, 6.0]$, we also tune for the best target return within range $[0.5, 1.5]$ for each tasks to test CFG's best performance.

Monte Carlo sampling from selections: For Monte Carlo sampling from selections (MCSS), N selections are firstly sampled from an unconditional generative model as candidates. Then these candidates are evaluated with a learnt critic for the selection of the optimal one. One advantage for MCSS is that, it do not rely on any task-specific hyperparameters for inference, such as the guidance strength w in CFG and CG, and target return in CFG. However, it needs to sample $N - 1$ more candidates during each decision making step, and requires more computation.

B IMPLEMENTATION DETAILS

B.1 MODEL ARCHITECTURE

Planner: Our code is based on CleanDiffuser (Dong et al., 2024b). We examined U-Net (Ronneberger et al., 2015) and Transformer (Vaswani et al., 2017) as the neural network backbone for all the diffusion planners. Specifically, we keep consistent with the implementation of U-Net1D (Janner et al., 2022), with 5 kernel size, $(1, 2, 2, 2)$ for channel multiplication, 32 base channels on MuJoCo, Kitchen and Maze2D, and 64 base channels on AntMaze. For Transformer, we use DiT1D (Peebles & Xie, 2023; Dong et al., 2024c), with hidden dimension of 256, head dimension of 32, 2 DiT blocks on MuJoCo, Kitchen and Maze2D, and 8 DiT blocks on AntMaze. All the planner diffusion models are trained with the Adam (Kingma & Ba, 2014) optimizer with learning rate of $3e-4$, batch size of 128, for 1M gradient steps. All the diffusion models in this work are trained to predict the noise. However, for U-Net1D experiments on Kitchen, the diffusion planner to predict the clean estimation, because it could achieve quite better performance.

Inverse dynamics: We used an MLP-based diffusion model as the inverse dynamic model, whose input is the current state and the planned next-state; and the output is the action to execute. It is implemented with a 3-layer MLP with additional 2-layer embedding layer and trained with $1M$ gradient steps. All the inverse dynamic models are trained with the Adam (Kingma & Ba, 2014)

optimizer with learning rate of $3e-4$, batch size of 128. We found that the using diffusion model as inverse dynamics show similar performance with vanilla MLP inverse dynamics.

Critic: We also implemented two types of critic models for guided sampling. The first type has the architecture of the U-Net1D for the planner, with a linear output layer to produce the critic value. The second type is a 2 blocks vanilla transformer, with hidden dimension of 256 as the value function, with a linear projection head on the first token output. We trained all the critic model using the Adam (Kingma & Ba, 2014) optimizer with learning rate of $3e-4$, batch size of 128. The model will be trained with 200K gradient steps, if it is a clean critic model [1]. Otherwise, it is trained for 1M gradient steps.

B.2 Diffusion solver

We use DDIM (Song et al., 2020) of temperature 1.0 for planner diffusion sampling, and DDPM with temperature of 0.5 for inverse dynamic action sampling. The sampling temperature is introduced to reduce sampling randomness (Ajay et al., 2022).

B.3 Dataset Pre-Processing

Diffusion policy baselines (Chen et al., 2023; Wang et al., 2023b; Hansen-Estruch et al., 2023) commonly learns policy, Q functions, and value functions using a temporal difference manner, on standard transitions $(\boldsymbol{s}_t, \boldsymbol{a}_t, \boldsymbol{s}_{t+1}, r_t)$. Admittedly, diffusion planners often require careful dataset pre-processing, including horizon padding, planning strides, return calculation, and truncation-termination handling. An unsuccessful sequential dataset pre-processing may greatly reduce the planning ability of diffusion planners. Most planning tasks are usually sparse rewarded, and how optimality is defined, combined with different temporal credit assignment methods is also important. For MuJoCo and Kitchen, we use discount factor $\gamma = 0.997$. For Maze2D and AntMaze, we use IQL-maze (Kostrikov et al., 2021) reward shaping methods for temporal credit assignment in navigation planning tasks, where an -1 penalty is always applied to agent during every timestep.

B.4 Full hyper-parameters

Table 2 displays the hyperparameters and default choices in our work.

[1] A clean critic model is only trained on clean input data, while a noised critic model is trained using noised data using the diffusion model's noise schedule

Table 2: Configuration Settings

Settings	**Default**	**Choices**
Guidance Type	MCSS	[MCSS, CG, CFG, None]
State-Action Generation	Separate	[Joint, Separate]
Advantage Weighting	True	[True, False]
Inverse Dynamic	Diffusion	[Diffusion, Regular]
Time Credit Assignment	discount=0.997	[discount=0.997, IQL-maze]
Planner Net. Backbone	Transformer	[Transformer, UNet]
UNet Channels Mult	(1, 2, 2, 2)	(1, 2, 2, 2)
UNet Base Channels	32	[16, 32, 64]
Transformer Hidden	256	256
Transformer Block	2	[2, 4, 6, 8]
Planner Solver	DDIM	[DDIM, DDPM]
Planner Sampling Steps	20	20
Planner Training Steps	1000000	1000000
Planner Temperature	1	1
MCSS Candidates	50	[1, 20, 50]
Planning Horizon	32	[4, 32, 40]
Planning Stride	1	[1, 2, 4, 5, 15, 25]
Inverse Dynamics Net. Backbone	MLP	MLP
Inverse Dynamics Hidden	256	256
Inverse Dynamics Solver	DDPM	DDPM
Inverse Dynamics Sampling Steps	10	10
Inverse Dynamics Training Steps	1000000	1000000
Policy Temperature	0.5	0.5

C EXTENSIVE RESULTS

The following plots show the attention weights in different DDIM denoising steps in each task. We can see that a long-term dependency is generally existing in the Transformer.

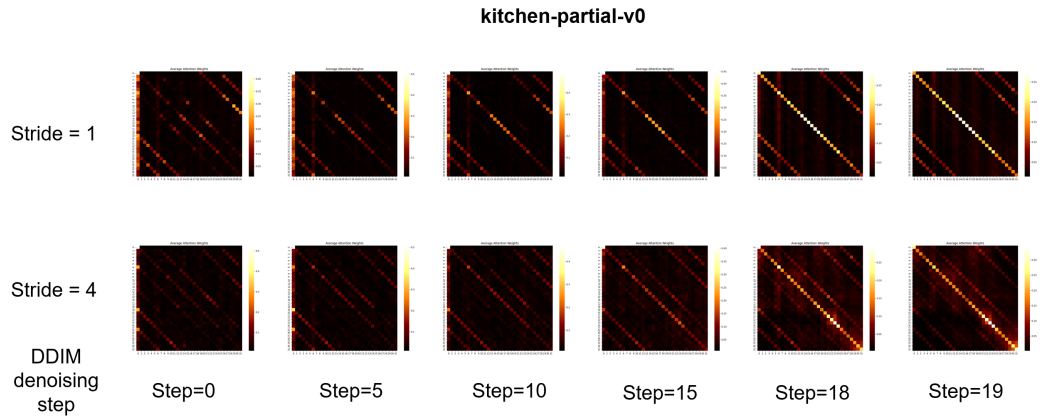

Figure 9: Attention weights (averaged on multi-heads) of the first Transformer layer of DV on the Kitchen-Partial-v0 dataset.

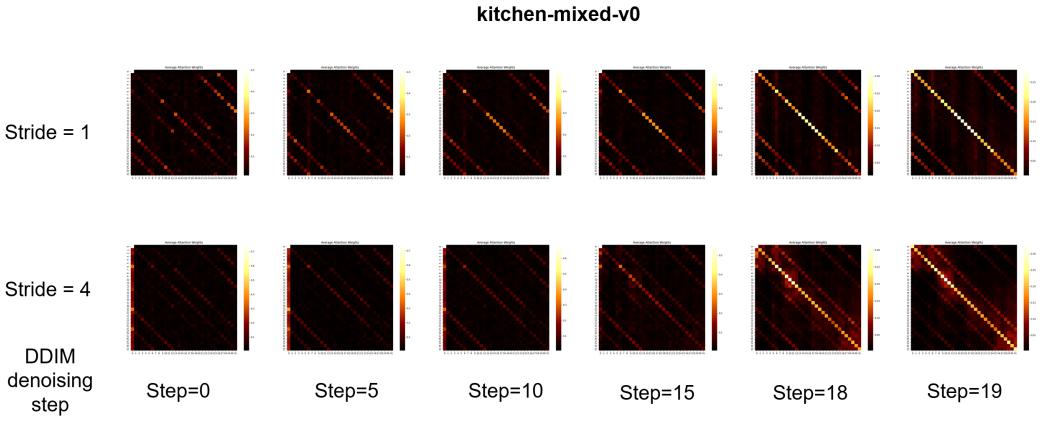

Figure 10: Attention weights (averaged on multi-heads) of the first Transformer layer of DV on the Kitchen-Mixed-v0 dataset.

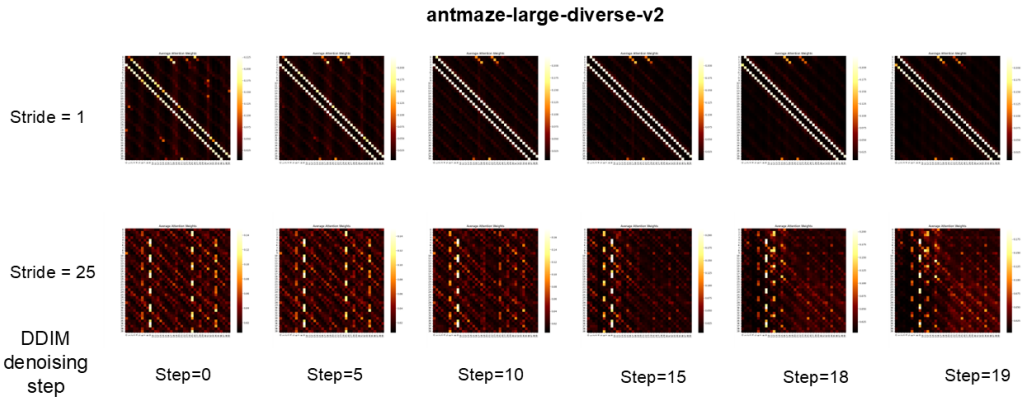

Figure 11: Attention weights (averaged on multi-heads) of the first Transformer layer of DV on the AntMaze-Large-Diverse-v2 dataset.

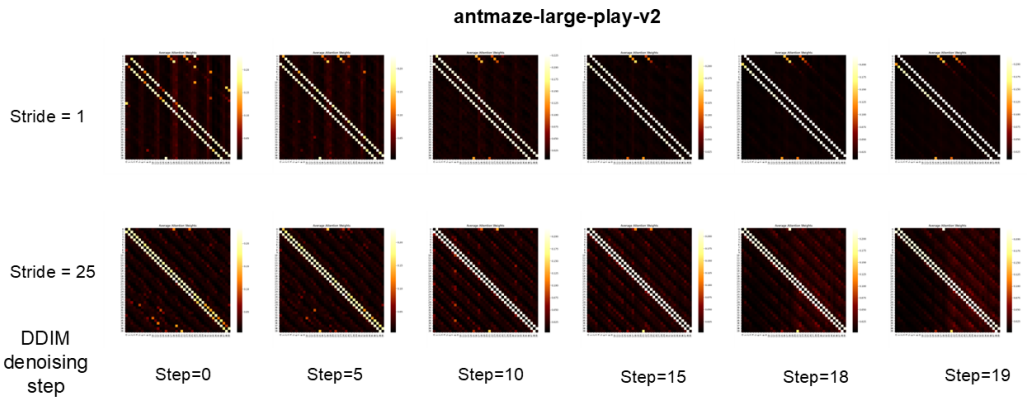

Figure 12: Attention weights (averaged on multi-heads) of the first Transformer layer of DV on the AntMaze-Large-Play-v2 dataset.

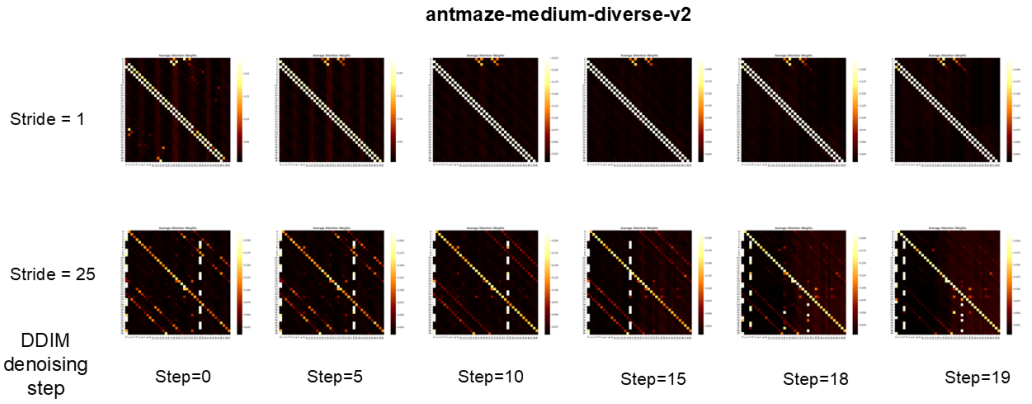

Figure 13: Attention weights (averaged on multi-heads) of the first Transformer layer of DV on the AntMaze-Medium-Diverse-v2 dataset.

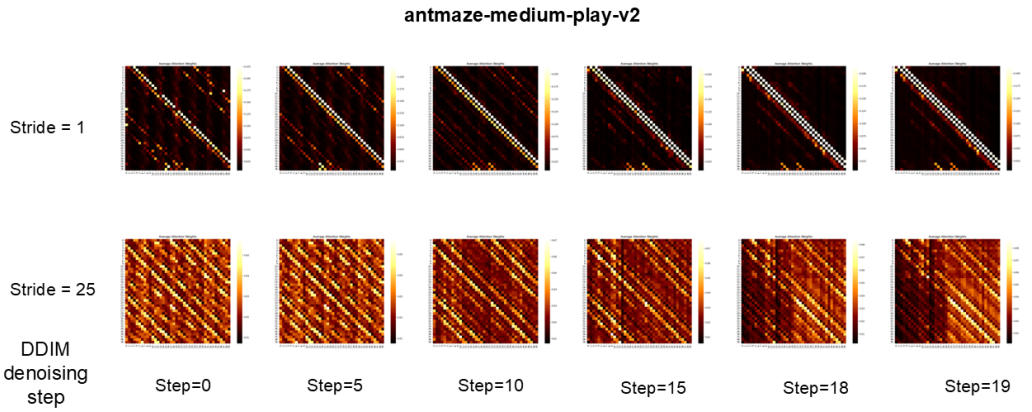

Figure 14: Attention weights (averaged on multi-heads) of the first Transformer layer of DV on the AntMaze-Medium-Play-v2 dataset.

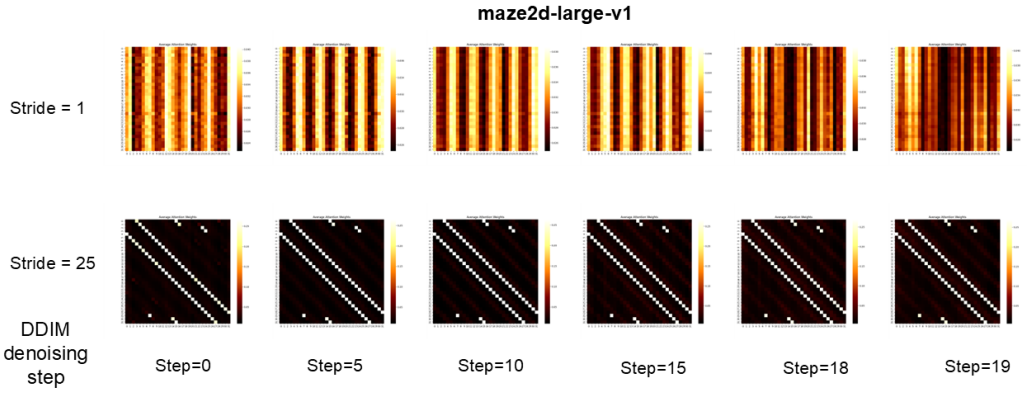

Figure 15: Attention weights (averaged on multi-heads) of the first Transformer layer of DV on the Kitchen-Mixed-v0 dataset.

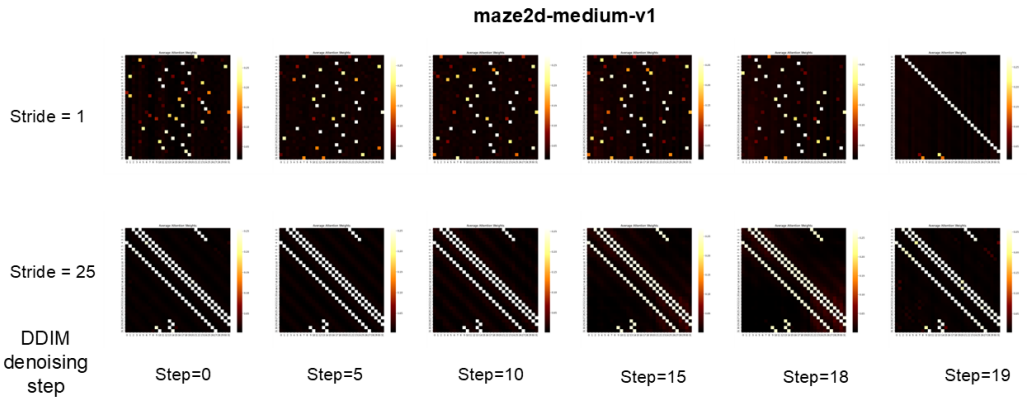

Figure 16: Attention weights (averaged on multi-heads) of the first Transformer layer of DV on the Maze2D-Large-v1 dataset.

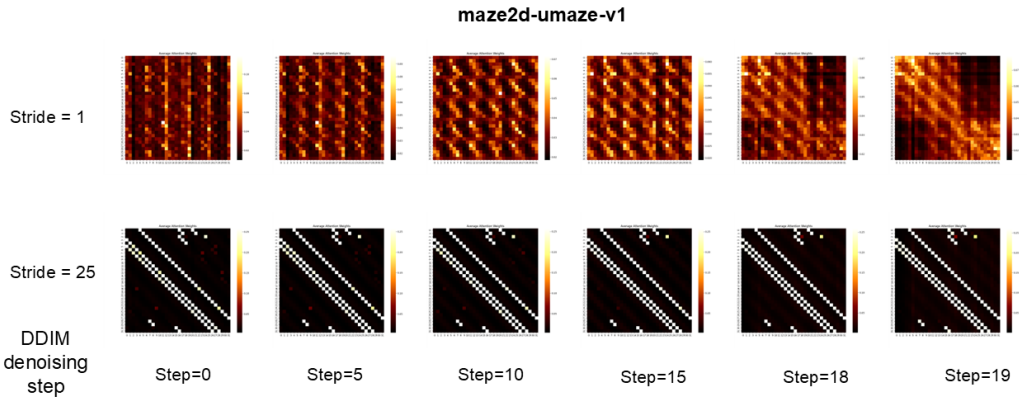

Figure 17: Attention weights (averaged on multi-heads) of the first Transformer layer of DV on the Maze2D-medium-v1 dataset.

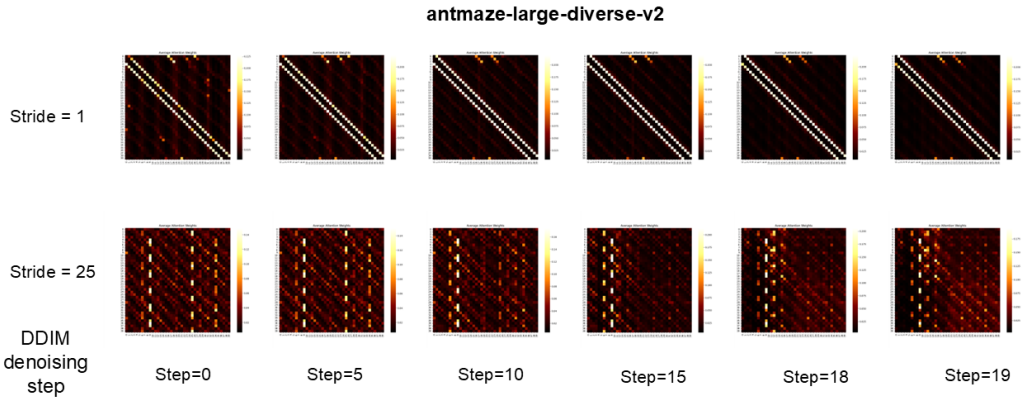

Figure 18: Attention weights (averaged on multi-heads) of the first Transformer layer of DV on the Maze2D-UMaze-v1 dataset.

Table 3: Normalized performance of various offline-RL methods. Data are Mean ± Standard Error (if available).

		IL	None-diffusion Polices			Diffusion Policies						Diffusion Planners				
Dataset	**Environment**	BC	BCQ	CQL	IQL	SfBC	DQL	DQL*	IDQL	IDQL*	CEP	Diffuser	AdaptDiffuser	DD	HD	**DV**
Medium-Expert	HalfCheetah	35.8	64.7	62.4	86.7	92.6 ± 0.5	96.8 ± 0.3	95.5 ± 0.1	95.9	91.3 ± 0.6	93.5 ± 0.3	88.9 ± 0.3	89.6 ± 0.8	90.6 ± 1.3	92.5 ± 0.3	92.7 ± 0.3
Medium-Replay	HalfCheetah	38.4	38.2	46.2	44.2	37.1 ± 1.7	47.8 ± 0.3	47.9 ± 0.0	45.9	46.5 ± 0.3	47.6 ± 1.4	37.7 ± 0.5	38.3 ± 0.9	39.3 ± 4.1	115.3 ±1.1	45.8 ± 0.1
Medium	HalfCheetah	36.1	40.7	44.4	47.4	45.9 ± 2.2	51.1 ± 0.5	52.3 ± 0.2	51.0	51.5 ± 0.1	54.1 ± 0.4	42.8 ± 0.3	44.2 ± 0.6	49.1 ± 1.0	107.1 ± 1.1	50.4 ± 0.0
Medium-Expert	Hopper	111.9	110.9	98.7	91.5	108.6 ± 2.1	111.1 ± 1.3	111.1 ± 0.4	108.6	110.1 ± 0.7	108.0 ± 2.5	103.3 ± 1.3	111.6 ± 2.0	111.8 ± 1.8	46.7 ± 0.2	110.0 ± 0.5
Medium-Replay	Hopper	11.3	33.1	48.6	94.7	86.2 ± 9.1	101.3 ± 0.6	101.6 ± 0.0	92.1	99.4 ± 0.1	96.9 ± 2.6	93.6 ± 0.4	92.2 ± 1.5	100.0 ± 0.7	99.3 ± 0.3	91.9 ± 0.0
Medium	Hopper	29.0	54.5	58.0	66.3	57.1 ± 4.1	90.5 ± 4.6	96.5 ± 1.3	65.4	70.1 ± 2.0	98.0 ± 2.6	74.3 ± 1.4	96.6 ± 2.7	79.3 ± 3.6	84.0 ± 0.6	83.6 ± 1.2
Medium-Expert	Walker2d	6.4	57.5	111.0	109.6	109.8 ± 0.2	110.1 ± 0.3	111.6 ± 0.0	112.7	110.6 ± 0.0	110.7 ± 0.6	106.9 ± 0.2	108.2 ± 0.8	108.8 ± 1.7	38.1 ± 0.7	109.2 ± 0.0
Medium-Replay	Walker2d	11.8	15.0	26.7	73.9	65.1 ± 5.6	95.5 ± 1.5	98.2 ± 0.1	85.1	89.1 ± 2.4	84.4 ± 4.1	70.6 ± 1.6	84.7 ± 3.1	75.0 ± 4.3	94.7 ± 0.7	85.0 ± 0.5
Medium	Walker2d	6.6	53.1	79.2	78.3	77.9 ± 2.5	87.0 ± 0.9	86.8 ± 0.2	82.5	88.1 ± 0.4	86.0 ± 0.7	79.6 ± 0.6	84.4 ± 2.6	82.5 ± 1.4	84.1 ± 2.2	82.8 ± 0.1
Average		31.9	52.0	63.9	77.0	75.6	87.9	**89.1**	82.1	84.1	86.6	77.5	83.3	81.8	84.6	83.5
Mixed	Kitchen	47.5	8.1	51.0	51.0	45.4 ± 1.6	62.6 ± 5.1	55.1 ± 1.58	66.5	66.5 ± 4.1	–	52.5 ± 2.5	51.8 ± 0.8	75.0 ± 0.0	71.7 ±2.7	73.6 ± 0.1
Partial	Kitchen	33.8	18.9	49.8	46.3	47.9 ± 4.1	60.5 ± 6.9	65.5 ± 1.38	66.7	66.7 ± 2.5	–	55.7 ± 1.3	55.5 ± 0.4	56.5 ± 5.8	73.3 ± 1.4	94.0 ± 0.3
Average		40.7	13.5	50.4	48.7	46.7	61.6	60.3	66.6	66.6	–	54.1	53.7	65.8	72.5	**83.8**
Antmaze-Large	Diverse	0.0	2.2	61.2	47.5	45.5 ± 6.6	56.6 ± 7.6	70.6 ± 3.7	67.9	40.0 ± 11.4	64.8 ± 5.5	27.3 ± 2.4	8.7 ± 2.5	0.0 ± 0.0	83.6 ± 5.8	80.0 ± 1.8
Antmaze-Large	Play	0.0	6.7	53.7	39.6	59.3 ± 14.3	46.4 ± 8.3	81.3 ± 3.1	63.5	48.7 ± 4.7	66.6 ± 9.8	17.3 ± 1.9	5.3 ± 3.4	0.0 ± 0.0	–	76.4 ± 2.0
Antmaze-Medium	Diverse	0.0	0.0	15.8	70.0	82.0 ± 3.1	78.6 ± 10.3	82.6 ± 3.0	84.8	83.3 ± 5.0	83.8 ± 3.5	2.0 ± 1.6	6.0 ± 3.3	4.0 ± 2.8	88.7 ± 8.1	87.4 ± 1.6
Antmaze-Medium	Play	0.0	0.0	14.9	71.2	81.3 ± 2.6	76.6 ± 10.8	87.3 ± 2.7	84.5	67.3 ± 5.7	83.6 ± 4.4	6.7 ± 5.7	12.0 ± 7.5	8.0 ± 4.3	–	89.0 ± 1.6
Average		0.0	2.2	36.4	57.1	67.0	64.6	80.5	75.2	59.8	74.7	13.3	8.0	3.0	–	**83.2**
Maze2D	Large	5	6.2	12.5	58.6	74.4 ± 1.7	–	186.8 ± 1.7	90.1	–	–	123	167.9 ± 5.0	–	128.4 ± 3.6	203.6 ± 1.4
Maze2D	Medium	30.3	8.3	5.0	34.9	73.8 ± 2.9	–	152.0 ± 0.8	89.5	–	–	121.5	129.9 ± 4.6	–	135.6 ± 3.0	150.7 ± 1.0
Maze2D	Umaze	3.8	12.8	5.7	47.4	73.9 ± 6.6	–	140.6 ± 1.0	57.9	–	–	113.9	135.1 ± 5.8	–	155.8 ± 2.5	136.6 ± 1.3
Average		13.0	9.1	7.7	47.0	74.0		159.8	79.2			119.5	144.3		139.9	**163.6**

Table 4: The effect of guided sampling algorithms for DV, with different planning strides. In "Stride x/y", x is for Kitchen, and y is for Maze2D & AntMaze. Data are Mean ± Standard Error over 500 episode seeds.

		MCSS				CFG			
Dataset	**Environment**	Stride 1	Stride 2/5	Stride 4/15	Stride 8/25	Stride 1	Stride 2/5	Stride 4/15	Stride 8/25
Mixed	Kitchen	67.2 ± 0.3	74.2 ± 0.1	73.6 ± 0.1	–	72.7 ± 0.2	78.6 ± 0.1	72.4 ± 0.1	–
Partial	Kitchen	87.8 ± 0.6	88.3 ± 0.4	94.0 ± 0.3	–	95.9 ± 0.4	98.6 ± 0.3	95.2 ± 0.6	–
Average		77.5	81.3	83.8	–	84.3	88.6	83.8	–
Antmaze-Large	Diverse	72.4 ± 1.4	2.6 ± 0.1	71.2 ± 2.0	80.0 ± 1.8	54.4 ± 0.6	46.5 ± 0.1	6.4 ± 0.1	67.4 ± 0.3
Antmaze-Large	Play	61.2 ± 1.5	18.2 ± 0.5	76.2 ± 0.9	76.4 ± 2.0	60.8 ± 0.8	0.4 ± 0.0	59.4 ± 0.3	56.4 ± 0.5
Antmaze-Medium	Diverse	58.8 ± 1.5	24.2 ± 0.8	86.2 ± 1.6	87.4 ± 1.6	57.1 ± 0.6	5.0 ± 0.1	33.0 ± 0.8	49.0 ± 0.7
Antmaze-Medium	Play	38.8 ± 1.5	73.2 ± 1.5	83.8 ± 1.9	89.0 ± 1.6	55.9 ± 0.8	51.3 ± 0.7	28.7 ± 0.4	29.4 ± 0.5
Average		57.8	29.6	79.4	83.2	57.1	25.8	31.9	50.6
Maze2D	Large	168.2 ± 2.0	188.5 ± 1.6	203.6 ± 1.4	198.1 ± 1.5	15.1 ± 1.8	29.6 ±1.9	174.6 ± 2.3	42.0 ± 2.4
Maze2D	Medium	127.1 ± 1.4	141.3 ± 1.2	150.7 ± 1.0	151.4 ± 0.9	31.8 ± 1.7	97.8 ± 2.2	75.7 ± 2.1	153.4 ± 4.2
Maze2D	Umaze	131.8 ± 1.3	117.7 ± 1.6	136.6 ± 1.3	133.1 ± 1.2	21.6 ± 2.4	114.1 ± 2.7	30.2 ± 2.4	58.7 ± 2.5
Average		142.4	149.2	163.6	160.9	22.8	80.5	93.5	84.7
		CG				None			
Dataset	**Environment**	Stride 1	Stride 2/5	Stride 4/15	Stride 8/25	Stride 1	Stride 2/5	Stride 4/15	Stride 8/25
Mixed	Kitchen	64.0 ± 0.4	65.9 ± 0.4	61.3 ± 0.4	–	63.5 ± 0.4	63.5 ± 0.4	54.2 ± 0.3	–
Partial	Kitchen	58.9 ± 0.5	58.7 ± 0.6	58.4 ± 0.5	–	65.4 ± 0.5	56.0 ± 0.5	49.7 ± 0.5	–
Average		61.5	62.3	59.9	–	64.5	59.8	52.0	–
Antmaze-Large	Diverse	79.1 ± 1.3	35.3 ± 1.5	20.6 ± 1.1	77.2 ± 1.3	73.1 ± 1.4	16.8 ± 1.6	11.6 ± 1.4	78.2 ± 1.8
Antmaze-Large	Play	64.9 ± 1.5	12.2 ± 0.9	8.6 ± 0.8	73.8 ± 1.4	58.6 ± 1.5	30.8 ± 2.0	0.2 ± 0.1	69.8 ± 2.0
Antmaze-Medium	Diverse	71.6 ± 1.4	57.3 ± 1.5	67.3 ± 1.4	59.0 ± 1.5	67.2 ± 1.4	57.0 ± 2.2	61.6 ± 2.1	55.0 ± 2.2
Antmaze-Medium	Play	50.6 ± 1.5	61.0 ± 1.5	78.3 ± 1.3	75.3 ± 1.4	39.6 ± 1.5	60.8 ± 2.1	67.0 ± 2.1	70.0 ± 2.0
Average		66.6	41.5	43.7	71.3	59.6	41.4	35.1	68.3
Maze2D	Large	148.6 ± 2.9	142.1 ± 2.9	131.4 ± 2.6	174.1 ± 2.6	68.1 ± 3.0	45.2 ± 2.8	42.6 ± 2.7	47.5 ± 2.6
Maze2D	Medium	110.1 ± 2.2	113.3 ± 2.2	123.2 ± 2.1	126.9 ± 2.2	60.8 ± 2.3	61.9 ± 2.3	41.5 ± 2.2	47.3 ± 2.3
Maze2D	Umaze	80.4 ± 2.4	64.3 ± 2.4	67.6 ± 2.4	81.0 ± 2.4	47.6 ± 2.4	38.9 ± 2.4	27.5 ± 2.4	35.3 ± 2.4
Average		113.0	106.6	107.4	127.3	58.8	48.7	37.2	43.4

Table 5: Changing denoising network backbone for DV, with different planning strides. In "Stride x/y", x is for Kitchen, and y is for Maze2D & AntMaze. Data are Mean ± Standard Error over 500 episode seeds.

		Transformer (DiT1D)				U-Net (U-Net1D)			
Dataset	**Environment**	Stride 1	Stride 2/5	Stride 4/15	Stride 8/25	Stride 1	Stride 2/5	Stride 4/15	Stride 8/25
Mixed	Kitchen	67.2 ± 0.3	74.2 ± 0.1	73.6 ± 0.1	–	11.6 ± 0.5	35.2 ± 0.5	38.4 ± 0.8	–
Partial	Kitchen	87.8 ± 0.6	88.3 ± 0.4	94.0 ± 0.3	–	12.4 ± 0.5	28.8 ± 0.6	10.8 ± 0.5	–
Average		77.5	81.3	83.8		12.0	32.0	24.6	
Antmaze-Large	Diverse	72.4 ± 1.4	2.6 ± 0.1	71.2 ± 2.0	80.0 ± 1.8	53.7 ± 1.5	59.9 ± 1.5	76.7 ± 1.3	68.0 ± 1.4
Antmaze-Large	Play	61.2 ± 1.5	18.2 ± 0.5	76.2 ± 0.9	76.4 ± 2.0	53.4 ± 1.5	48.3 ± 1.5	80.8 ± 1.2	72.7 ± 1.4
Antmaze-Medium	Diverse	58.8 ± 1.5	24.2 ± 0.8	86.2 ± 1.6	87.4 ± 1.6	27.9 ± 1.4	55.5 ± 1.5	85.8 ± 1.1	81.1 ± 1.2
Antmaze-Medium	Play	38.8 ± 1.5	73.2 ± 1.5	83.8 ± 1.9	89.0 ± 1.6	28.5 ± 1.4	66.2 ± 1.4	81.0 ± 1.2	81.9 ± 1.2
Average		57.8	29.6	79.4	83.2	40.9	57.5	81.1	75.9
Maze2D	Large	168.2 ± 2.0	188.5 ± 1.6	203.6 ± 1.4	198.1 ± 1.5	172.5 ± 1.9	168.7 ± 2.2	193.1 ± 1.5	189.7 ± 1.5
Maze2D	Medium	127.1 ± 1.4	141.3 ± 1.2	150.7 ± 1.0	151.4 ± 0.9	140.0 ± 1.1	138.7 ± 1.1	145.9 ± 1.1	146.6 ± 1.0
Maze2D	Umaze	131.8 ± 1.3	117.7 ± 1.6	136.6 ± 1.3	133.1 ± 1.2	126.4 ± 1.4	120.0 ± 1.6	126.5 ± 1.4	121.4 ± 1.4
Average		142.4	149.2	163.6	160.9	146.3	142.5	155.2	152.6

Table 6: The impact of action generation method for DV, with different planning strides. In "Stride x/y", x is for Kitchen, and y is for Maze2D & AntMaze. Data are Mean ± Standard Error over 500 episode seeds.

		Separate				Joint			
Dataset	**Environment**	Stride 1	Stride 2/5	Stride 4/15	Stride 8/25	Stride 1	Stride 2/5	Stride 4/15	Stride 8/25
Mixed	Kitchen	67.2 ± 0.3	74.2 ± 0.1	73.6 ± 0.1	–	60.8 ± 0.4	62.9 ± 0.4	56.6 ± 0.6	–
Partial	Kitchen	87.8 ± 0.6	88.3 ± 0.4	94.0 ± 0.3	–	43.8 ± 0.7	53.7 ± 0.8	41.2 ± 0.7	–
Average		77.5	81.3	83.8		52.3	58.3	48.9	
Antmaze-Large	Diverse	72.4 ± 1.4	2.6 ± 0.1	71.2 ± 2.0	80.0 ± 1.8	49.9 ± 1.5	0.6 ± 0.2	0.2 ± 0.1	7.3 ± 0.8
Antmaze-Large	Play	61.2 ± 1.5	18.2 ± 0.5	76.2 ± 0.9	76.4 ± 2.0	56.7 ± 1.5	0.4 ± 0.2	0.1 ± 0.1	3.7 ± 0.5
Antmaze-Medium	Diverse	58.8 ± 1.5	24.2 ± 0.8	86.2 ± 1.6	87.4 ± 1.6	36.3 ± 1.5	2.5 ± 0.4	0.3 ± 0.1	6.3 ± 0.7
Antmaze-Medium	Play	38.8 ± 1.5	73.2 ± 1.5	83.8 ± 1.9	89.0 ± 1.6	34.0 ± 1.4	2.7 ± 0.5	3.7 ± 0.6	27.8 ± 1.4
Average		57.8	29.6	79.4	83.2	44.2	1.6	1.1	11.3
Maze2D	Large	168.2 ± 2.0	188.5 ± 1.6	203.6 ± 1.4	198.1 ± 1.5	187.0 ± 1.6	202.6 ± 1.4	202.9 ± 1.5	198.5 ± 1.6
Maze2D	Medium	127.1 ± 1.4	141.3 ± 1.2	150.7 ± 1.0	151.4 ± 0.9	141.4 ± 1.1	143.7 ± 1.1	156.0 ± 0.9	153.8 ± 0.9
Maze2D	Umaze	131.8 ± 1.3	117.7 ± 1.6	136.6 ± 1.3	133.1 ± 1.2	124.9 ± 1.6	139.8 ± 1.2	146.3 ± 1.1	141.1 ± 1.2
Average		142.4	149.2	163.6	160.9	151.1	162.0	168.4	164.5